A Theoretical Improvement of a Stirling Engine PV Diagram

N.M. Dehelean, L.M. Dehelean, E.-C. Lovasz and D. Perju

Mechanical Engineering Faculty, "Politehnica" University of Timisoara, 300222 Timisoara, Romania; e-mail: {nicolae.dehelean, liana.dehelean, erwin.lovasz, dan.perju}@mec.upt.ro

Abstract. Power efficiency of Stirling engine is low due to different causes. One of them is the displacement function of compression piston. This is pseudo-sinusoidal and is performed by a slider-crank mechanism. The thermo-dynamic functions should require a special displacement function for compression piston. Focusing on this request the paper proposes a new dwell mechanism.

Key words: Stirling engine, slider-crank mechanism, linkage drive mechanism, displacement and torque functions

1 On the Drive Mechanism for an α-Stirling Engine

The PV diagram of an α-Stirling engine (Figure 1) is far away from an ideal PV diagram (Figure 2). The principle schema of the α-Stirling engine is shown in Figure 3. It could be observed that the engine has two crank rod mechanisms, one from compression cylinder and the other for expansion cylinder. The displacement functions for both pistons (cylinders) are of approximately sin shape, as it is shown in Figure 4. The majority of the mechanisms used to drive the Stirling engines are crank-rod mechanisms. In [10] there is a schema of low-temperature differential solar Stirling engine powered by a flat-plate solar collector without regenerator shown in Figure 5. A modified slider-crank mechanism is analyzed in [2]; its schema is shown in Figure 6.

In Figure 7 it is shown the schematics of a rhombic drive with power piston connected to the upper and displacer to the lower section. This mechanism is analyzed in [8]. In the configuration shown, the left crank will turn clockwise and the right crank counter clockwise in order to achieve proper phase lag between expansion and compression space. They turn at the same angular velocity which can be accomplished by two intermeshing counter-rotating gears.

In [7] a calculator is made available online dedicated to optimize the solution for bowtie drives with unsymmetric sections. The schema of the mechanism is shown in Figure 8. It might have more choices than necessary to achieve design objectives

D. Pisla et al. (eds.), *New Trends in Mechanism Science:Analysis and Design*, Mechanisms and Machine Science 5, DOI 10.1007/978-90-481-9689-0_70,
© Springer Science+Business Media B.V. 2010

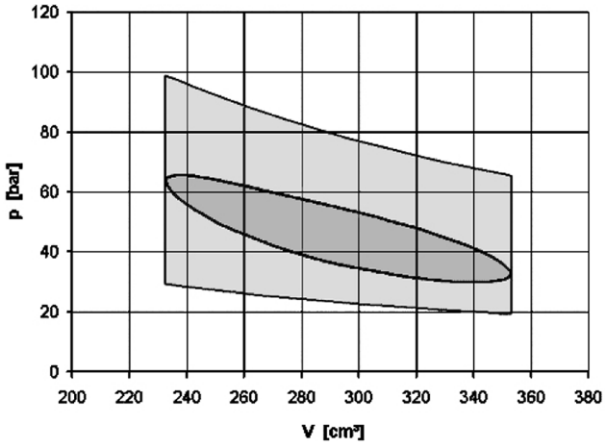

Fig. 1 Real Stirling PV diagram.

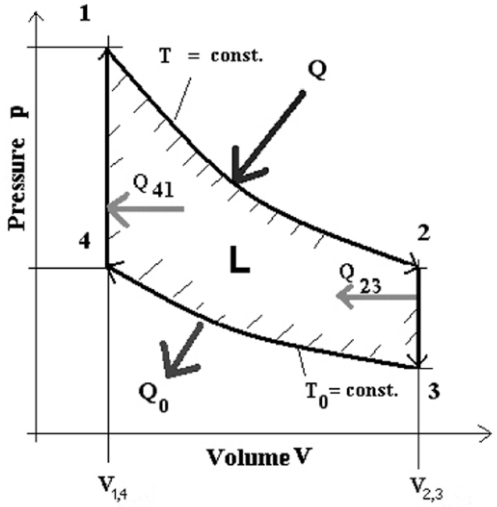

Fig. 2 Ideal Stirling PV diagram.

like: a swept-volume ratio between expansion and compression space of about 1, volumetric phase lag of about 90°, and minimal sidewise motion of the connection points 4 and 4′.

The slider-crank mechanism is part of the cause to the deficient PV diagram of a Stirling engine that uses it as a drive mechanism [1]. In [6] a calculator is made available online dedicated to a four bar mechanism for a Stirling engine as shown in Figure 9.

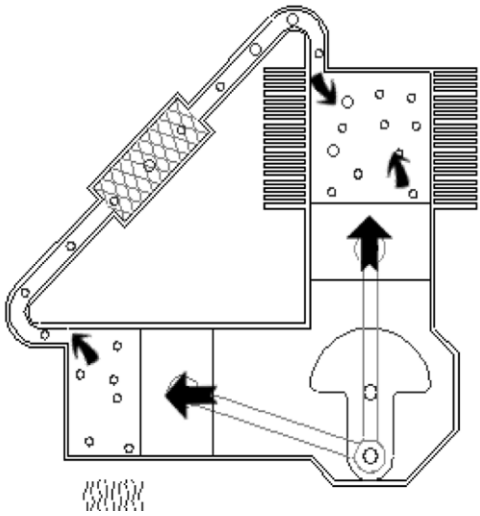

Fig. 3 Schema of the α Stirling engine.

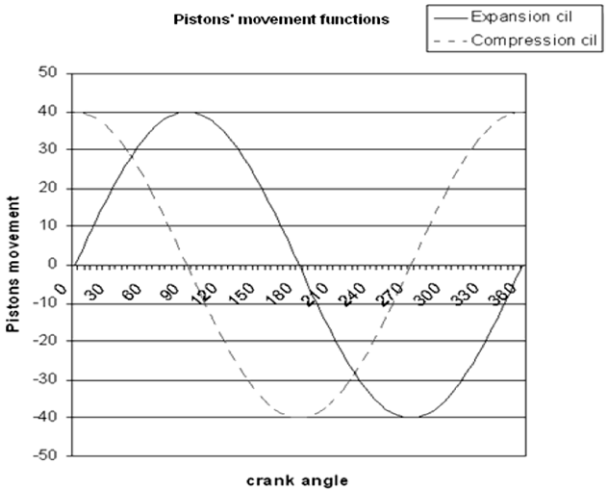

Fig. 4 The displacement functions.

2 A New Mechanism

The low efficiency of α-Stirling engine is proved by the PV diagram. This statement shoves the engine developers to improve the work characteristics in order to rise-up the engine efficiency. The main way to achieve this task is to improve the engine characteristics. There are a lot of mechanisms species that could be used to obtain a dwell movement necessary to the compression cylinder. It could be use-

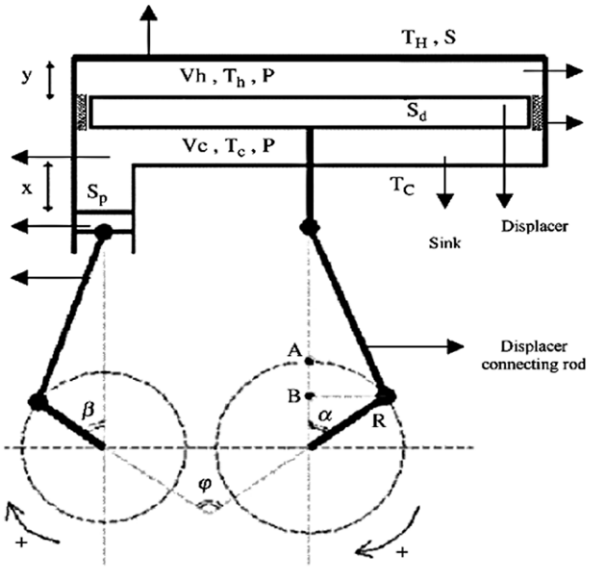

Fig. 5 Schema of differential solar engine.

ful a mechanism able to perform a dwell during the whole period of expansion. The dwell of the compression piston has to enlarge the active area of the PV diagram. As a consequence it is expected an efficiency improvement. This request could be very well accomplished by a cam mechanism. But this one is too large, too complicated, expensive and unreliable.

A linkage could be more reliable than cam mechanism despite the fact that the cam mechanism is more precise. The paper is focused on a dwell mechanism as a linkage one.

A good mechanism was proposed in [5] and the scheme is shown in Figure 10. The reference $x0y$ axes are placed according to the Schmidt Analysis [9]. Schmidt has made the classical Stirling Analysis in 1871. Using the same reference it can replace the sin function of compression cylinder, in the Schmidt Analysis by a new displacement function, in order to develop a new isothermal analysis of the engine. But this one is not good enough regarding the phases of the two pistons. In order to improve this situation a mechanism as shown in Figure 11 was proposed in [3].

The analysis of the dwell mechanism begun in [3] and it reveals the expected displacement functions $y_C(t)$ and $y_E(t)$ and the phase relation between them. The proper phase relation demonstrates that the mechanism is good for the application that it is focused on. Second, it must show that $y_E(t)$ has a dwell large enough level, in accordance with the expansion stroke time of the expansion cylinder.

Implementing the displacement functions from [3] in a computer program and proceeds to a numerical derivation it obtains the velocity and the acceleration functions. All these functions are shown in diagram Figure 12.

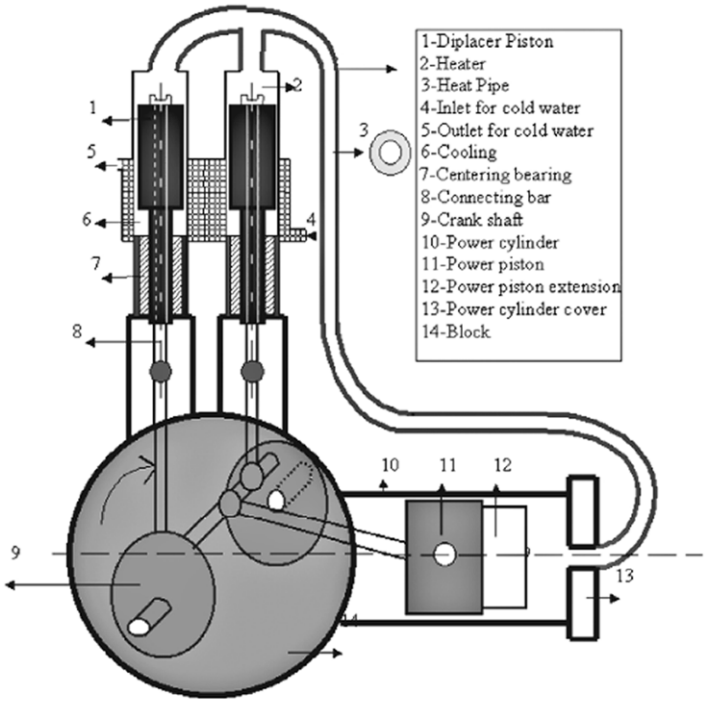

Fig. 6 Engine with two displacer pistons

The reference $x0y$ axes are placed in accordance with the Schmidt Analysis [9]. It should be noted that the sense of the crank rotation is in accordance with the classical Schmidt Analysis calculus. Some of the initial dimensions are given as follows: θ is the crank angle, proportional to time; V_{clc} is the clearance volume; V_{swc} is the swept volume; D_C is the cylinder diameter; $y_C(t)$ is the displacement of compression piston; $y_E(t)$ is the displacement of expansion piston.

The parameters in equations (1) are necessary to obtain the value of $y_{C\min}$.

$$V_{clc} = \min\{V_C\}; \quad \max\{V_C\} = V_{clc} + V_{swc}$$
$$V_C = V_{clc} + 0.5 \cdot V_{swc}(1 + \cos\theta) \tag{1}$$

$$Y_{C\min} = \frac{V_{clc}}{\pi\left(\frac{D_C}{2}\right)^2} \tag{2}$$

$y_{C\min}$ (equation 2) and h_1 (equation 3) are necessary to establish the dimensional structure of entire mechanism;

$$\vec{h_1} = \overrightarrow{O_1A} + \vec{AC} - \overrightarrow{y_{C\min}} \tag{3}$$

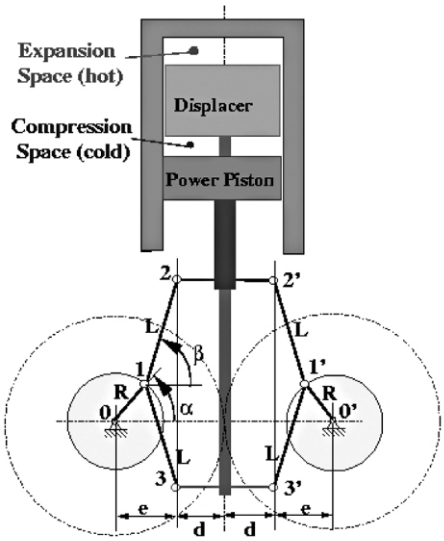

Fig. 7 Rhombic drive mechanism.

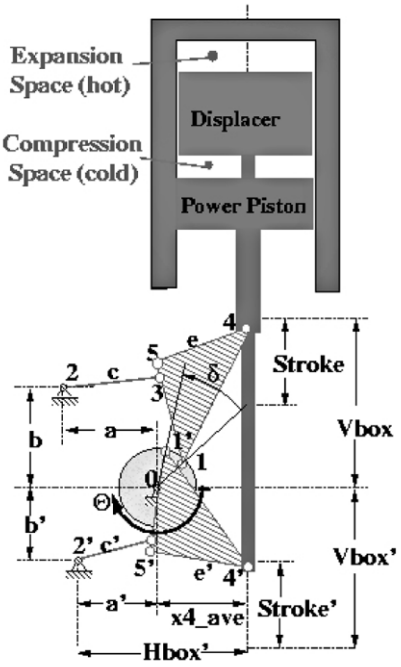

Fig. 8 Unsymmetric sections mechanism.

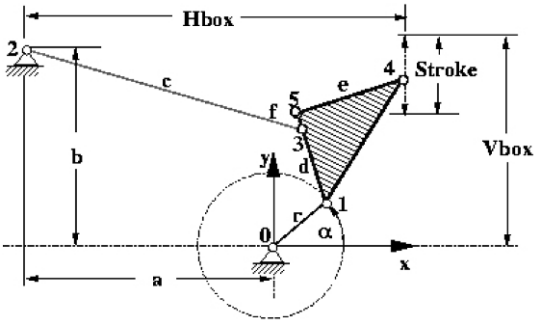

Fig. 9 A four bar mechanism.

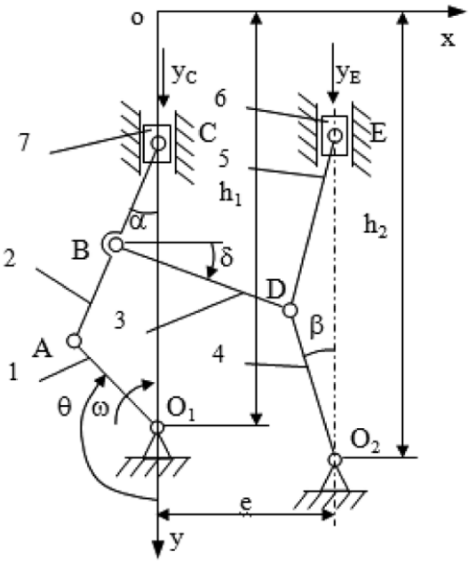

Fig. 10 Dwell mechanism.

Figure 12 shows the two displacement functions and the velocity and acceleration only for the compression piston. It is observed that the mechanism does not perform a perfect dwell, but the angle of the dwell is more important. The dwell angle is from about 220 to 310°. So, $\Delta\theta \approx 90°$.

The new displacement function $y_C(t)$ will be inserted in Schmidt Analysis, instead of sin relation.

For example the third equation in (1) from Schmidt Analysis has to be improved by replacing the term $0.5V_{swe} \cdot \cos(\theta + \delta)$ by $y_C(t)$. But function $y_C(t)$ does not have an analytical expression so the replacement could be done in a computer program.

$$V_e = V_{cle} + 0.5V_{swe}(1 + \cos(\theta + \delta)) \tag{4}$$

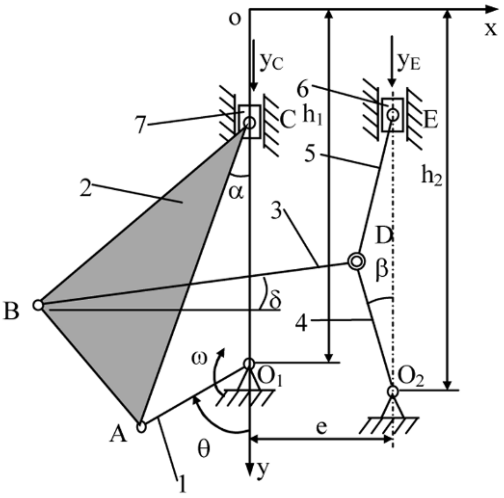

Fig. 11 New dwell mechanism.

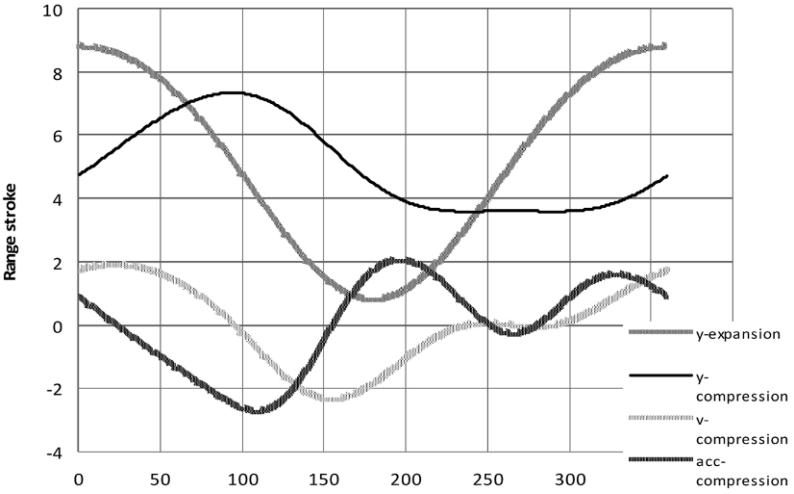

Fig. 12 Displacement, velocity and acceleration.

3 Torque New Dwell Mechanism Calculus

The torque calculus starts from the equivalent calculus in [4] and the added scheme is shown in Figure 13. This calculus is more detailed, rigorous and complete than the previous one [4]. It contains the equilibrium equations of the element (2) of the linkage, which are implemented in the computer program to obtain the diagram of the torque shown in Figure 14.

$$F_3 = \frac{2F_6 \cdot \tan\beta}{\cos\delta}; \quad \tan\delta = \frac{h_2 - y_B - R_2 \cdot \cos\beta}{x_B + R_2 \cdot \sin\beta - e} \tag{5}$$

The main equation of calculus is the generic torque equation (6). The set of equations (7) represents the geometrical relations among the main geometric and auxiliary points on linkage schema (Figure 13). The equation system (8) represents the equilibrium relations of the element (2).

$$T = R_{A_{2R}} \cdot R_{Crod} \cdot \sin\theta - R_{A_{1R}} \cdot R_{Crod} \cos\theta \tag{6}$$

$$BS = \frac{h}{\cos\alpha}; \quad TS = h \cdot \tan\alpha; \quad CS = b - b_1 - h \cdot \tan\alpha; \quad SU = CS \cdot \sin\alpha$$
$$CU = CS \cdot \cos\alpha; \quad CQ = h_1 + R_{Crod} \cdot \cos\theta; \quad s = BS + SU \tag{7}$$

where R_{Crod} is the crank radius, R_2 is the secondary crank radius and b, b_1, h, h_1, h_2, s are the geometrical dimensions of the linkage.

$$\begin{cases} R_C + R_{A1} - F_3 \cdot \cos\delta = 0 \\ F_7 + F_3 \cdot \sin\delta - R_{A2} = 0 \\ F_3 \cdot \cos\delta (CQ - CU) + F_3 \cdot \sin\delta (s - R_{Crod} \cdot \sin\theta) - R_C \cdot CQ = 0 \end{cases} \tag{8}$$

In the equation system (8) the first two equations represent $(\sum F)_x = 0$ and $(\sum F)_y = 0$. The last equation represents $(\sum M)_A = 0$.

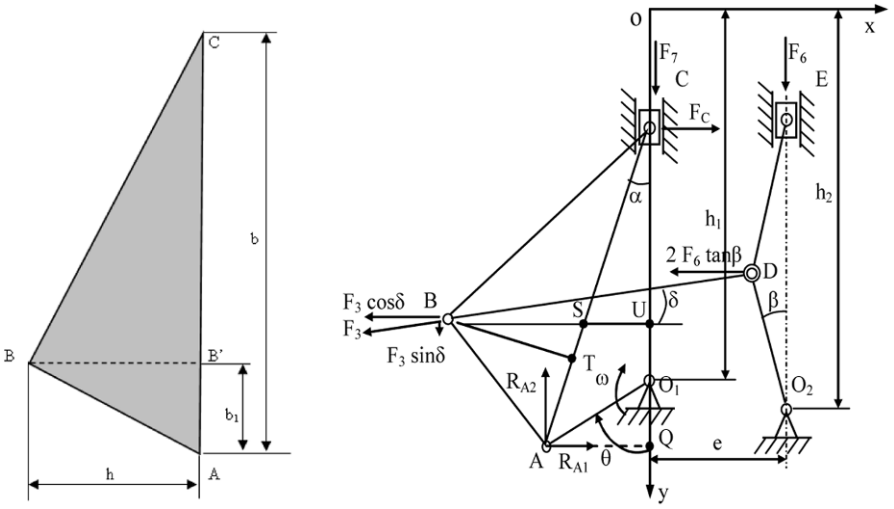

Fig. 13 External forces scheme.

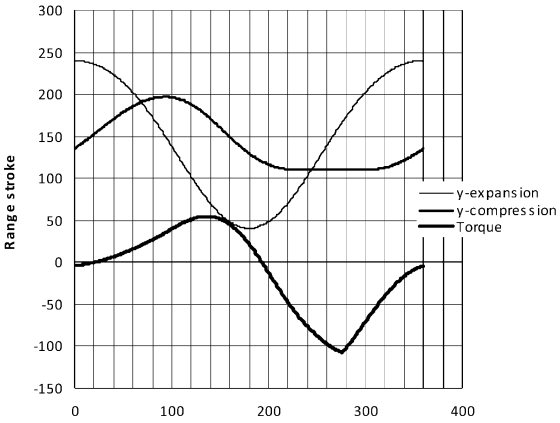

Fig. 14 Torque diagram.

In order to view the configuration of the torque at element (1) it implements equations (1) to system equation (8) into the computer program that was used in [4]. The torque diagram is shown in Figure 14. It could be observed that torque presents a positive maximum along the dwell angle of the compression cylinder (in the torque diagram the sign (+) is under the 0x axis).

4 Conclusions

The torque diagram configuration is a reliable argument to sustain the attempt to improve the PV diagram of classical Stirling engine (with two slide-crank mechanisms, see Figure 3) using the proposed linkage (Figure 11). Movement, velocity and acceleration functions of the compression cylinder (piston) prove that the proposed linkage is able to perform a dwell in a proper phase position. Torque function of the crank presents a maximum point along the dwell angle of the compression cylinder. The two diagrams prove that the paper makes a step award to improve the Stirling engine design.

References

1. Ataera, E.O. and Karabulutb, H., Thermodynamic analysis of the V-type Stirling-cycle refrigerator, *International Journal of Refrigeration*, 28:183–189, 2005.
2. Batmaz, I. and Süleyman, Ü., Design and manufacturing of a V-type Stirling engine with double heaters, *Applied Energy*, 85:1041–1049, 2008.
3. Dehelean, N.M. and Ciupe, V., The analisis of a dwell mechanism for α-Stirling engine. In *Proceedings of the 10th IFToMM International Symposium on Science of Mechanisms and Machines, SYROM'09*.

4. Dehelean, N.M., Ciupe, V. and Lovasz, E.-C., A digital model of a dwell mechanism for alpha Stirling engine. In *Proceedings of the 10th IFToMM International Symposium on Science of Mechanisms and Machines, SYROM'09*.
5. Dehelean, N.M., Ciupe, V. and Maniu, I., A new Mechanism to syncrhonize α-Stirling engine, *Scientific Bulletin of "Politehnica" University of Timisoara*, 53(67), S1:81–84, 2008.
6. Herzog, Z., Web-based program "4bar", available from http://mac6.ma.psu.edu/stirling/drives/4bar/4bar.html.
7. Herzog, Z., Web-based program "bowtie", available from http://mac6.ma.psu.edu/stirling/drives/bowtie/index.html.
8. Herzog, Z., Analysis of the symmetric rhombic drive, available from http://mac6.ma.psu.edu/stirling/drives/beta_rhombic/index.html.
9. Herzog, Z., The Schmidt analysis of Stirling engines, available from http://mac6.ma.psu.edu/stirling/simulations/isothermal/schmidt.html, 2008.
10. Tavakolpoura, A.R., Zomorodiana, A. and Golneshan, A., Simulation, construction and testing of a two-cylinder solar Stirling engine powered by a flat-plate solar collector without regenerator, *Renewable Energy*, 33:77–87, 2008.